JOURNAL OF THE ENGINEERING MECHANICS DIVISION

ENDOCHRONIC THEORY OF INELASTICITY AND FAILURE OF CONCRETE

By Zdeněk P. Bažant,[1] M. ASCE and Parameshwara D. Bhat[2]

INTRODUCTION

Two types of stress-strain relations for concrete have been extensively studied: (1) Plastic (1,36,43,44); and (2) hypoelastic (18,23,24,25,27,31,32,38,40,44,47). However, the plasticity theory, which has been developed primarily for metals with a well-pronounced yield plateau, is foreign to concrete; satisfactory hardening rules and formulations of the inelastic dilatancy, of the hydrostatic pressure sensitivity, of the strain-softening tendency, and of the cyclic straining, have not yet been found. In the hypoelastic model, unloading behavior cannot be easily represented, and to model stress-induced anisotropy without prohibitive complexities, the dependence of the incremental moduli upon the stress components must be simplified to a linear tensor polynomial which incorrectly implies the strains at maximum stress to be infinite. An entirely different approach to materials in which the inelastic strain accumulates gradually has been introduced by Valanis (45) (see also Ref. 30). It consists in characterizing the inelastic strain accumulation by a certain scalar parameter, z, called intrinsic time, whose increment is a function of strain increments. An independent variable of this type appears quite naturally as a length parameter of the trajectory traced by the states of the material in a six-dimensional space whose coordinates are the strain components (22,33,37). However, it was Valanis who was apparently first to realize the tremendous possibilities offered by this approach in a practical description of material behavior and developed for metals an endochronic theory which correctly predicts stain-hardening, unloading diagrams, effect of pretwist on axial behavior, contraction of hysteresis loops in cyclic loading, and the effect of strain rate.

Extension of the endochronic theory to concrete requires several novel

Note.—Discussion open until January 1, 1977. To extend the closing date one month, a written request must be filed with the Editor of Technical Publications, ASCE. This paper is part of the copyrighted Journal of the Engineering Mechanics Division, Proceedings of the American Society of Civil Engineers, Vol. 102, No. EM4, August, 1976. Manuscript was submitted for review for possible publication on December 18, 1974.

[1]Prof. of Civ. Engrg., Northwestern Univ., Evanston, Ill.
[2]Grad. Research Asst., Northwestern Univ., Evanston, Ill.

concepts, which were proposed in general terms in 1974 (3) and described numerically in a summary fashion in 1975 (12). They include: (1) The sensitivity of intrinsic time increments (measuring the accumulation of inelastic strain) to hydrostatic pressure; (2) inelastic dilatancy due to shear straining; (3) description of strain-softening tendency; (4) dependence of tangent moduli on dilatancy (not on stress or strain tensor); and, if long-time nonlinear creep should be modeled, also (5) introduction of more than one intrinsic time. The purpose

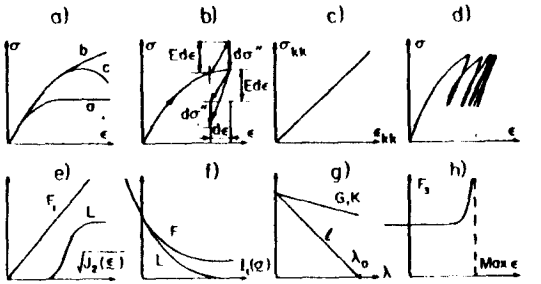

FIG. 1.—Diagrams of Some Characteristic Functions

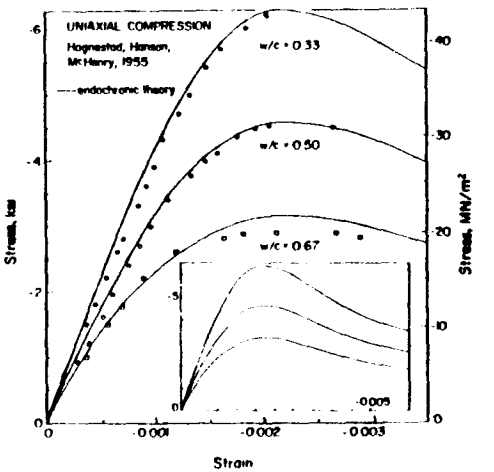

FIG. 2.—Fit of Uniaxial Stress-Strain Data (20) for Concretes

of this paper is to develop these concepts in detail and demonstrate agreement with experimental data, virtually over the full range of essential material properties known at present.

INTRINSIC TIME

It is instructive to begin with a heuristic demonstration. Consider the uniaxial stress-strain relation for the Maxwell solid, $d\epsilon = d\sigma/E + \sigma\, dt/EZ_1$, in which t = time; ϵ = strain; σ = stress; E = elastic modulus; Z_1 = constant; and try

what happens if dt is replaced with $d\epsilon$. Then, multiplying by $E/d\epsilon$, one gets a linear differential equation for σ as a function of ϵ, $d\sigma/d\epsilon + \sigma/Z_1 = E$. The solution for the initial condition $\sigma = 0$ at $\epsilon = 0$ is $\sigma = EZ_1(1 - e^{-\epsilon/Z_1})$, which is a curve resembling the inelastic stress-strain diagram [curve a, Fig. 1(*a*)]. Furthermore, to model unloading, try replacing $d\epsilon$ with $dz = |d\epsilon|$, so that $d\sigma = Ed\epsilon - d\sigma''$ with $d\sigma'' = \sigma|d\epsilon|/Z_1$. Let loading be suddenly reversed into unloading. At that moment $Ed\epsilon$ changes sign to negative, while $d\sigma''$ does not change sign. This is graphically represented in Fig. 1(*b*) and it is clear that the unloading branch is steeper than the loading branch. This is a very simple way to model irreversibility at unloading, the salient aspect of all inelasticity.

Thus, it is of interest to analyze the preceding arbitrary manipulations in a rational way and a three-dimensional form. Their basic feature is that the actual time, t, has been replaced by a variable depending on strain. In this light, it is natural to seek an independent variable z, called intrinsic time, such that dz is a function of strain increments $d\epsilon_{ij}$. In a material exhibiting time-dependent response, dz must also be a function of dt. Assuming that the development of inelastic strain is gradual (which excludes ideally plastic yielding), $(dz)^s$ as a function of $d\epsilon_{ij}$ and dt (with an appropriate exponent, s) must be continuous and smooth, so that it may be expanded in a tensorial power series in $d\epsilon_{ij}$ and dt, i.e.

$$(dz)^s = p^{(0)} + p^{(1)}_{ij}\,d\epsilon_{ij} + p^{(1)}_4\,dt + p^{(2)}_{ijkl}\,d\epsilon_{ij}\,d\epsilon_{kl} + p^{(2)}_{ij4}\,d\epsilon_{ij}\,dt + p^{(2)}_{44}(dt)^2$$
$$+ p^{(3)}_{ijklmn}\,d\epsilon_{ij}\,d\epsilon_{kl}\,d\epsilon_{mn} + \ldots \qquad (1)$$

The latin indices refer to the components in cartesian coordinates x_i, $i = 1, 2, 3$, and repeated indices imply summation. Since dz must vanish as $d\epsilon_{ij} \to 0$ and $dt \to 0$, it is necessary that $p^{(0)} = 0$. Furthermore, z may never decrease, or else the non-negativeness of the energy dissipation could not be ensured. Therefore, it is necessary that $p^{(1)}_{ij} = 0$ and that coefficients $p^{(2)}_{ijkl}$, $p^{(2)}_{ij4}$, $p^{(2)}_{44}$ describe a positive definite quadratic form in seven variables $d\epsilon_{11}$, $d\epsilon_{12}$, ..., $d\epsilon_{33}$, dt. Dividing Eq. 1 by $(dt)^s$ one obtains

$$\left(\frac{dz}{dt}\right)^s = p^{(1)}_4(dt)^{1-s} + \left[p^{(2)}_{ijkl}\frac{d\epsilon_{ij}}{dt}\frac{d\epsilon_{kl}}{dt} + p^{(2)}_{ij4}\frac{d\epsilon_{ij}}{dt} + p^{(2)}_{44}\right](dt)^{2-s} + \ldots \qquad (2)$$

in which no terms may be infinite. One possibility of meeting this condition is to set $s = 1$; but then all quadratic terms are negligibly small and $dz = p^{(1)}_4\,dt$, which is of no interest. Thus, $p^{(1)}_4 = 0$. The remaining possible choice is $s = 2$. The terms of order higher than two are negligible with regard to the quadratic terms.

To satisfy the conditions of isotropy, the quadratic form in Eq. 1 may involve solely the invariants of the tensor $[d\epsilon_{ij}] = d\underline{\epsilon}$. The third invariant, being cubic, cannot appear and the most general tensorially invariant quadratic form that is positive definite is

$$(dz)^2 = P_0 J_2(d\underline{\epsilon}) + [P_1 I_1(d\underline{\epsilon}) + P_2\,dt]^2 + P_3(dt)^2 \qquad (3)$$

provided that P_0 and P_3 are non-negative. The term $J_2(d\underline{\epsilon})$ = second invariant of the deviator of tensor $d\underline{\epsilon}$. Furthermore, for instantaneous ($dt = 0$), purely volumetric deformations [for which $J_2(\underline{\epsilon}) = 0$] the inelastic strain is negligible, and so dz must vanish. Hence, $I_1(d\underline{\epsilon})$ $(= d\epsilon_{kk})$ cannot be present. Thus,

$(dz)^2$ must reduce to the expression, $P_0 J_2(d\underline{\epsilon}) + P_3(dt)^2$, and noting that the coefficients in this expression ought to depend in general on the state variables, it is convenient to rewrite this expression as

$$(dz)^2 = \left(\frac{d\zeta}{Z_1}\right)^2 + \left(\frac{dt}{\tau_1}\right)^2; \quad d\zeta = f_1(\xi, \underline{\epsilon}, \underline{\sigma})\,d\xi \qquad (4)$$

$$\text{with} \quad d\xi = \sqrt{J_2(d\underline{\epsilon})} = \sqrt{\frac{1}{2}\,de_{ij}\,de_{ij}} \qquad (5)$$

in which Z_1 = constant; and $e_{ij} = \epsilon_{ij} - \delta_{ij}\epsilon$ = deviator of the strain tensor [$\epsilon = (1/3)\epsilon_{kk}$ = volumetric strain; δ_{ij} = Kronecker delta]; f_1 = hardening-softening function. Variable ξ will be called distorsion measure, so as to reflect the fact that $d\xi$ depends only on the deviatoric strain increments. Coefficient τ_1 has the dimension of time and may be called relaxation time. For loading durations much less than τ_1, the term, dt/τ_1, in Eq. 4 may be neglected and the intrinsic time is independent of time per se, as required. Note also that for uniaxial strain and for $dt = 0$, Eqs. 4 and 5 yield $dz \sim |d\epsilon|\sqrt{1/3}$, which is proportional to $|d\epsilon|$ as considered at the beginning. Eqs. 4 and 5 with f_1 independent of $\underline{\epsilon}$ and $\underline{\sigma}$ have been proposed by Valanis (45) (without the preceding derivation).

Previous authors have frequently used the term "damage" to describe the changes produced in the microstructure of concrete by microcracking, yet damage has never been expressed quantitatively. It is proposed that ζ provides a possible measure of damage.

Stress-Strain Relations

Attention will first be restricted to short-time deformations for which creep may be neglected. To satisfy the condition of isotropy, the incremental stress-strain relations may be split into one relation between the increments of volumetric components, $\epsilon = (1/3)\epsilon_{kk}$ and $\sigma = (1/3)\sigma_{kk}$, and another relation between the increments of deviatoric components, e_{ij} and s_{ij}. Expressing the strain increments as a sum of elastic increments and inelastic increments de''_{ij}, $d\epsilon''$, one has

$$de_{ij} = \frac{ds_{ij}}{2G} + de''_{ij}; \quad de''_{ij} = \frac{s_{ij}}{2G}\,dz \qquad (6a)$$

$$d\epsilon = \frac{d\sigma}{3K} + d\epsilon''; \quad d\epsilon'' = d\lambda + \frac{\sigma}{3K}\frac{dt}{\tau_1} + d\epsilon^0 \qquad (6b)$$

in which ϵ^0 = stress-independent inelastic strain (thermal dilatation plus shrinkage); and λ = inelastic dilatancy (to be distinguished from the elastic dilatancy or Poynting effect). Inclusion of inelastic dilatancy is one of the basic generalizations as compared with Valanis' endochronic theory for metals (45). Note that, for short-time deformations of concrete, $d\epsilon''$ does not depend upon σ because under pure volumetric stress the time-independent inelastic strain may be neglected [see Fig. 1(*c*)], which agrees with the absence of microcracking. The time-dependent volumetric strain (creep) is represented by the term, $\sigma\,dt/3K\tau_1$, which, by contrast, must involve σ because creep is linear at low stress. The use of K in this term assures that the Poisson ratio for low-stress

creep is the same as that for elastic strains. The time-dependent volumetric strain (creep) is represented by the term, $\sigma\,dt/3K\tau_1$, which, by contrast, must involve σ because creep is linear at low stress. The use of K in this term assures that the Poisson ratio for low-stress creep is the same as that for elastic strains.

A refinement will be required for lightweight concrete, in which a further mechanism, i.e., the collapse of pores and localized crushing of the material between the pores also contributes to inelastic strain. Then, the expression for $d\epsilon''$ in Eq. 6*b* may have to be augmented by a term of the type $(\sigma/3K)\,dz'$, in which dz' = another intrinsic time such that $dz' \sim |d\epsilon| \sim |I_1(d\underline{\epsilon})|$. Under extremely high pressures, this might be also necessary for normal-weight concretes.

A fundamental difference from plasticity theory is the absence of the yield function and the normality rule. However, normality relations are satisfied by endochronic theories in a sense similar to viscoelasticity (30).

Strain-Hardening.—As the inelastic strain accumulates, its further increase gets harder to be produced, for the potential locations of stress peaks in the microstructure are getting exhausted. This is best apparent in cyclic loading [Fig. 1(*d*)]. To account for this effect, coefficient f_1 in Eq. 4 must decrease as the inelastic strain accumulates, and because ζ is herein adopted as a measure of the accumulated inelastic strain (or damage), f_1 must decrease as ζ increases. To this effect, let

$$d\zeta = \frac{d\eta}{f(\eta)}; \quad d\eta = F(\underline{\epsilon}, \underline{\sigma})\,d\xi \qquad (7)$$

in which $f(\eta)$ = strain-hardening function = certain continuous monotonically increasing positive function; and $F(\underline{\epsilon}, \underline{\sigma})$, $= f(\eta)\, f_1(\xi, \underline{\epsilon}, \underline{\sigma})$, f_1 being given by Eq. 4. Eq. 7 may be integrated to yield $\zeta = \zeta(\eta)$, which again may be inverted to yield $\eta = \eta(\zeta)$, so that it would be equivalent to write $d\zeta = f_2(\zeta)\,d\eta$. Because $d\zeta$ is in Eq. 4 divided by arbitrary constant Z_1, there is no loss in generality to set $f(0) = 1$. The simplest possible choice is a linear expression, $f(\eta) = 1 + \beta_1\eta$ ($\beta_1 \geq 0$), which leads to $\zeta = \beta_1^{-1} \ln(1 + \beta_1\eta)$ and $\eta = (e^{\beta_1\zeta} - 1)/\beta_1$. This was applied with success to metals (45) and appears to be also satisfactory for concrete, with the exception of large values of η that arise under cyclic loading. The expression, $f(\eta) = 1 + \beta_1\eta + \beta_2\eta^2$ ($\beta_2 \geq 0$), seems to be acceptable up to about 10^6 load cycles. Parameters β_1 and β_2 have also considerable effect on the curvature of the stress-strain diagram at the peak. To ensure that after passing the peak the stress-strain curves continuously decline, hardening must be eliminated at large strain. For this purpose one may set

$$d\zeta = \frac{d\eta}{\left(1 + \dfrac{\beta_1\eta + \beta_2\eta^2}{1 + a_7 F_1}\right) F_2}; \quad F_2 = 1 + \frac{a_8}{\left(1 + \dfrac{a_9}{\eta^2}\right) J_2(\underline{\epsilon})} \qquad (8)$$

in which F_1 = function that governs strain-softening and is given in the sequel; a_7, a_8, a_9 = constants; and F_2 = function that is added so as to cause the cyclic stress loops at low cyclic deviator strains [low $J_2(\underline{\epsilon})$] to contract more strongly; this is needed only during the first few cycles, i.e., for small η, and

therefore a_9 is divided by η^2 in Eq. 8. For all other situations, $F_2 \approx 1$.

Strain-Softening and Hydrostatic Pressure Sensitivity.—If coefficient F in Eq. 7 were constant, then the uniaxial stress-strain diagram [for $f(\eta)$ as given] would approach an asymptote of positive slope [curve b, Fig. 1(*a*)] and the failure of the material could not be modeled. To obtain a gradual decrease of slope on approach to peak stress [curve c, Fig. 1(*a*)], the inelastic strain increments must be increased, which may be obtained by an increase in F as a function of ϵ; F will be called strain-softening function. [A function of η rather than $\underline{\epsilon}$ has been used for metals (46), but for concrete this would give too much softening in low-stress cyclic loading.]

Function F, however, serves also the important purpose of introducing the hydrostatic pressure sensitivity of concrete (2,35). This sensitivity results from the fact that hydrostatic pressure $p = -\sigma = -\sigma_{kk}/3$ inhibits the formation as well as the opening of microcracks and that the friction forces on closed microcrack surfaces are larger at higher p. Indeed, at very high p, microcracks cannot open, and so concrete (like rocks) becomes perfectly plastic.

In view of isotropy, F may depend on $\underline{\epsilon}$ only through the invariants, $I_1(\underline{\epsilon})$, $J_2(\underline{\epsilon})$, and $I_3(\underline{\epsilon})$. For further simplification, consider the special case when $J_2(\underline{\epsilon}) = 0$, i.e., $(\epsilon_1 - \epsilon_2)^2 + (\epsilon_2 - \epsilon_3)^2 + (\epsilon_3 - \epsilon_1)^2 = 0$ (ϵ_1, ϵ_2, and ϵ_3 being the principal strains); obviously, a zero value of $J_2(\underline{\epsilon})$ occurs only when $\epsilon_1 = \epsilon_2 = \epsilon_3 = \epsilon$, i.e., when the strain is purely volumetric. When ϵ is a compression ($\epsilon < 0$), no microcracks should be present, and noting that the dependence of F upon $\underline{\epsilon}$ is due to microcracking, and that $I_1(\underline{\epsilon})$ or $I_3(\underline{\epsilon})$ is not necessarily zero when $J_2(\underline{\epsilon}) = 0$, one must conclude that F may depend neither upon $I_1(\underline{\epsilon})$ nor upon $I_3(\underline{\epsilon})$. Therefore, at $\epsilon < 0$, F may depend only upon $J_2(\underline{\epsilon})$ which reflects the effect of microcracking. This dependence must disappear when p is very large, making concrete perfectly plastic. The dependence on p must fade when $J_2(\underline{\epsilon}) = 0$. ($I_1$ and I_3 = first and third invariants.)

For $\epsilon > 0$ or $\sigma > 0$ (tension) the cracking is, of course, possible even when $J_2(\underline{\epsilon}) = 0$, and the most simple way to express the tensile strain-softening is to postulate a dependence of F upon the maximum principal strain and stress, max ϵ and max σ. This is admissible because max ϵ and max σ depend only on the basic strain and stress invariants and are, therefore, invariants themselves.

The foregoing conditions for the strain softening function can be satisfied by an expression of the form

$$F(\underline{\epsilon}, \underline{\sigma}) = \left\{\frac{a_0}{1 - [a_6 I_3(\underline{\sigma})]^{1/3}} + F_1\right\} F_3 \qquad (9)$$

$$\text{with} \quad F_1 = \frac{a_2[1 + a_5 I_2(\underline{\sigma})]\sqrt{J_2(\underline{\epsilon})}}{\{1 - a_1 I_1(\underline{\sigma}) - [a_3 I_3(\underline{\sigma})]^{1/3}\}[1 + a_4 I_2(\underline{\sigma})\sqrt{J_2(\underline{\epsilon})}]} \qquad (10)$$

$$F_3 = 1 + \left[50\left(1 - \frac{\max\epsilon}{\epsilon_0}\right)\left(1 - \frac{\max\sigma}{f_t'}\right)\right]^{-3} \qquad (11)$$

in which $I_2(\underline{\sigma})$ = second stress invariant (i.e., $\sigma_1\sigma_2 + \sigma_2\sigma_3 + \sigma_3\sigma_1$ in terms of principal stresses) (I_1 and I_3 are negative for compression); a_0, a_1, ... a_6 = constants, of which a_1 must be such that $F(\underline{\epsilon}, \underline{\sigma})$ can never become negative prior to tensile failure; and f_t' = tensile strength.

Function F_3 in Eq. 9 [Fig. 1(*h*)] accounts for tensile failure. It equals unity except when the maximum principal strain or stress is very close to a certain fixed value, in which case it blows up to infinity, expressing the fact that the rate of microcracking greatly increases as the failure is approached. Thus, function F_3 is essentially equivalent to maximum tensile strain and stress cutoffs in the failure criterion. Alternatively, function F_3 can be left out of Eq. 9 if the inequalities, max $\epsilon < \epsilon_0$ and max $\sigma < f_t'$, are imposed as conditions of no failure. The strain cutoff is most likely appropriate for multiaxial stress states and also enables describing the fact that the tensile strength diminishes with load duration. However, to model failure when unloading after compression reaches into tensile stress at compressive strain, the stress cutoff is necessary.

The term with a_0 in Eq. 9 accounts for the plastic strain, which is independent of deviator strain [and thus of $J_2(\underline{\epsilon})$] and prevails under very high p. Parameter a_6 adjusts this term to avoid a too rapid decline of the slope of stress-strain curves at very high p; for all other situations, a_6 has a negligible effect. Parameter a_0 is needed mainly for adjusting the initial slope of triaxial curves. Function F_1 expresses the strain-softening due to microcracking, a mechanism that dominates when p is low. In fact, η can be split as $\eta = \eta_p + \eta_m$, in which η_p could be called measure of plastic slip and η_m measure of microcracking ($d\eta_m = F_1\, d\xi$). The appearance of $I_1(\underline{\sigma})$ in the expression for F_1 causes the softening due to $J_2(\underline{\epsilon})$ (microcracking) to disappear at high p. To control the relationship of biaxial and triaxial stress-strain curves to uniaxial ones, $I_2(\underline{\sigma})$ and $I_3(\underline{\sigma})$ (with parameters a_5, a_4, and a_3) are used in F_1 since they have the convenient properties that $I_2(\underline{\sigma})$ is zero only in uniaxial loading and $I_3(\underline{\sigma})$ is nonzero only in triaxial loading. Term $a_3 I_1(\underline{\sigma})$ in F_1 is needed mainly to adjust the triaxial response at medium hydrostatic pressure p. Since the difference between multiaxial and uniaxial tests is greater at larger strain, $I_2(\underline{\sigma})$ may be multiplied by $\sqrt{J_2(\underline{\epsilon})}$ (see Eq. 10). The associated parameters, a_4 and a_5, affect mainly the biaxial curves. Because the development of microcracking, as characterized by $J_2(\underline{\epsilon})$, makes strain-hardening impossible, terms $\beta_1\eta + \beta_2\eta^2$ must disappear at large $J_2(\underline{\epsilon})$, and this is achieved by placing F_1 in Eq. 8. If F_1 were absent from Eq. 8, the response curves would decline after the peak only briefly and then they would resume rising again and tend to infinity. With F_1, on the other hand, a steady decline after the peak and an approach to a horizontal asymptote are assured. The peak stress value is also strongly affected by Z_1 and a_2.

The fact that the intrinsic time increments depend not only upon $d\underline{\epsilon}$ and $\underline{\epsilon}$, but also upon $\underline{\sigma}$ (though not $d\underline{\sigma}$), represents a basic difference with respect to metals. It has been tried whether $I_1(\underline{\sigma})$ could be replaced by $I_1(\underline{\epsilon})$ in Eq. 10; but no acceptable fit of test data could then be obtained, chiefly for three reasons: Firstly, $I_1(\underline{\sigma})$ and $I_1(\underline{\epsilon})$ are not only produced by hydrostatic pressure, but also by uniaxial or biaxial loading. In these tests, as strain-softening begins to develop on approach to peak stress, $I_1(\underline{\epsilon})$ increases much faster than $I_1(\underline{\sigma})$, which would make the denominator in Eq. 10 too large and the peak stress in uniaxial tests too high as compared with triaxial tests. Secondly, on the strain-softening branch, $I_1(\underline{\sigma})$ decreases while $I_1(\underline{\epsilon})$ increases, which would disagree with the fact that microcracking is becoming more and more intense along this branch. Thirdly, when creep under constant hydrostatic pressure is considered, $I_1(\underline{\sigma})$ is constant while $I_1(\underline{\epsilon})$ grows, and so the use of $I_1(\underline{\epsilon})$ would

give a large increase in peak stress for a rapid uniaxial test performed after creep under hydrostatic stress, which is not observed in reality.

Inelastic Dilatancy.—This effect is in uniaxial compression tests manifested by the increase of Poisson ratio to and over 0.5 when failure is imminent. Because dilatancy originates from microcracking due to deviator strains, it must be governed by distorsion measure ξ. By intuitive arguments similar to those which led to Eq. 9, one may arrive at the expression $d\lambda = l(\lambda)L\{J_2(\underline{\epsilon}), I_1(\underline{\sigma}), \lambda\}\, d\xi$, in which l may be called dilatancy hardening function; and L, dilatancy softening function [Figs. 1(*e*)-1(*g*)]. The relation between λ and ξ is of the same type as the relation between ζ and ξ (Eq. 7), since $f(\eta)$, with $\eta = \eta(\zeta)$, is an implicit function of ζ. The following expression has been devised:

$$d\lambda = \left(1 - \frac{\lambda}{\lambda_0}\right) \frac{1}{1 - c_1' I_1(\underline{\sigma})} \left\{ \left(\frac{\lambda}{\lambda_0}\right)^2 + \left(\frac{J_2(\underline{\epsilon})}{c_2^2 + J_2(\underline{\epsilon})}\right)^2 \right\} c_0\, d\xi \quad \ldots\ldots (12)$$

in which c_0, c_1', c_2, λ_0 = material constants. Practical experience indicated that λ has a very profound effect on predicted behavior, especially on the cyclic load response (shape of the hysteresis loops) and on the Poisson ratio at cyclic load. Parameter λ_0 represents the maximum possible value to which λ gradually approaches. Such a maximum value must exist because there is a certain maximum volume that a concrete fully broken up into gravel can occupy. Presence of $I_1(\underline{\sigma})$ reflects the fact that dilatancy must vanish at high hydrostatic pressure, because no cracks can open. The term with $J_2(\underline{\epsilon})$ assures that there is no appreciable dilatancy in cyclic compression if strains are so low that there is no dilatancy in the first cycle, and that the dilatancy is quite pronounced but gradual when load cycles reach into high stress; $J_2(\underline{\epsilon})$ is used because it is the deviator strains that cause microcracking.

Dependence of G and K on Dilatancy.—Since the inelastic dilatancy consists in opening of microcracks, the incremental elastic moduli should decrease as λ grows. It is proposed that [Fig. 1(*g*)]:

$$G = G_0\left(1 - 0.25\frac{\lambda}{\lambda_0}\right); \quad K = K_0\left(1 - 0.25\frac{\lambda}{\lambda_0}\right) \quad \ldots\ldots\ldots\ldots (13)$$

in which G_0 and K_0 are the initial shear and bulk moduli:

$$G_0 = \frac{E_0}{2(1+\nu)}; \quad K_0 = \frac{E_0}{3(1-2\nu)} \quad \ldots\ldots\ldots\ldots\ldots\ldots (14)$$

E_0 = initial Young's modulus; and ν = Poisson ratio at low stress (elastic), $\nu \approx 0.18$. Coefficient 0.25 in Eq. 13 is deduced from the measurements of the speed of sound in uniaxially compressed specimens, which reveal a drop in speed of about 10%-20% shortly before failure (14,41). Making G and K dependent on a scalar, λ, circumvents the tremendous difficulties that inevitably arise in hypoelasticity when the incremental anisotropy due to the dependence of elastic moduli on a tensor, $\underline{\sigma}$, is considered (see Ref. 18). Nevertheless, some incremental anisotropy might have to be considered in a more accurate model, because microcracks do exhibit a statistically prevalent orientation that depends on the stress state. Choosing F and K to vary proportionally, the elastic Poisson ratio is assumed to be constant and the changes in the observed Poisson ratio are attributed solely to inelastic strains.

Time-Hardening Simplification for Creep.—If τ_1 in Eq. 4 were constant, the creep rate predicted by Eqs. 6 would not change, while in reality it decays roughly as the inverse of load duration. This fact may be approximately accounted for by making τ_1 increase with the load duration, $t - t_0$, t_0 being the instant of loading. This approximation, which may be called time-hardening, is widely used for approximate treatment of metal creep and is of the same nature as that in the rate-of-creep method for concrete creep (4,7). The time-hardening approximation is acceptable only if stress varies in time very slowly. A suitable expression is

$$\tau_1 = \tau_a + \tau_b(t - t_0) \quad \ldots\ldots\ldots\ldots\ldots\ldots\ldots\ldots\ldots\ldots \quad (15)$$

in which τ_a, τ_b = constants; τ_a affects mainly the early stages of creep; and τ_b, the long-time creep.

Physical Sources of Inelasticity.—From the preceding analysis it is clear that various terms in the constitutive law reflect the three mechanisms of inelastic deformations of concrete: (1) Microcracking due to the presence of aggregate; (2) plastic slip in cement gel; and (3) low stress-creep, which is probably due to microdiffusion of certain components of solids in cement gel (4,11). In a highly porous concrete under extreme hydrostatic pressure, crushing of pore walls may be added as a fourth mechanism, but this is not covered by the present theory.

Step-by-Step Numerical Integration of Structural Response

To solve structural analysis problems, the loads and enforced deformations are incremented in small steps and in each step the following algorithm, in which subscripts $r-1$ and r refer to the beginning and end of rth step, may be used (e.g., in conjunction with the finite element method):

1. Assume that those of increments $\Delta\sigma_{ij}$ and $\Delta\epsilon_{ij}$, which are not directly specified, are the same as those obtained in the previous step (for all elements of the structure). However, if there is a discontinuity of the prescribed loading path at stage $r-1$, assume them all to be zero. (In fact, zero values can be assumed as a rule, but more iterations are then required.)

2. Estimate mean values in the rth step as $\sigma_{ij,\,r-(1/2)} = \sigma_{ij,\,r-1} + (1/2)\Delta\sigma_{ij}$, $\epsilon_{ij,\,r-(1/2)} = \epsilon_{ij,\,r-1} + (1/2)\Delta\epsilon_{ij}$, and $\lambda_{r-(1/2)}$ (for all finite elements).

3. Evaluate $F(\underline{\xi},\underline{\sigma})_{r-(1/2)}$, $f(\eta)_{r-(1/2)}$, $G_{r-(1/2)}$, $K_{r-(1/2)}$, and $\tau_{1,\,r-(1/2)}$ (from Eqs. 8-15) and calculate $\Delta\xi$, $\Delta\eta$, $\Delta\zeta$, Δz, $\Delta\lambda$ (for all elements), and $\xi_{r-(1/2)}$ [$= \xi_{r-1} + (1/2)\Delta\xi$], $\eta_{r-(1/2)}$, ..., $\lambda_{r-(1/2)}$.

4. Calculate the volumetric and deviatoric components of tensors $\underline{\sigma}_{r-1}$, $\underline{\epsilon}_{r-1}$. Then evaluate inelastic stress increments $\Delta s''_{ij} = s_{ij,\,r-(1/2)}\,\Delta z$; $\Delta\sigma'' = 3K\Delta\lambda + \sigma_{r-(1/2)}\,\Delta t/\tau_{1,\,r-(1/2)} + 3K\Delta\epsilon^0$; and $\Delta\sigma''_{ij} = \Delta s''_{ij} + \delta_{ij}\Delta\sigma''$ (for all elements).

5. Denoting $\Delta s''_{ij} = 2G\Delta e''_{ij}$ and $\Delta\sigma'' = 3K\Delta\epsilon''$, the stress-strain relations (Eqs. 6) yield $2G_{r-(1/2)}\Delta e_{ij} = \Delta s_{ij} + \Delta s''_{ij}$, $3K_{r-(1/2)}\Delta\epsilon = \Delta\sigma + \Delta\sigma''$, which may be recast in the matrix form as $\Delta\underline{\sigma} + \Delta\underline{\sigma}'' = \underline{D}\Delta\underline{\epsilon}$, in which $\Delta\underline{\sigma}'' = [\Delta\sigma''_{ij}] = [\Delta s''_{ij} + \delta_{ij}\Delta\sigma''] =$ matrix of inelastic stresses. This form is

$$\begin{Bmatrix} \Delta\sigma_{11} + \Delta\sigma''_{11} \\ \Delta\sigma_{22} + \Delta\sigma''_{22} \\ \Delta\sigma_{33} + \Delta\sigma''_{33} \\ \Delta\sigma_{12} + \Delta\sigma''_{12} \\ \Delta\sigma_{23} + \Delta\sigma''_{23} \\ \Delta\sigma_{31} + \Delta\sigma''_{31} \end{Bmatrix} = \begin{bmatrix} D_1 & D_2 & D_2 & 0 & 0 & 0 \\ D_2 & D_1 & D_2 & 0 & 0 & 0 \\ D_2 & D_2 & D_1 & 0 & 0 & 0 \\ 0 & 0 & 0 & D_3 & 0 & 0 \\ 0 & 0 & 0 & 0 & D_3 & 0 \\ 0 & 0 & 0 & 0 & 0 & D_3 \end{bmatrix} \begin{Bmatrix} \Delta\epsilon_{11} \\ \Delta\epsilon_{22} \\ \Delta\epsilon_{33} \\ \Delta\epsilon_{12} \\ \Delta\epsilon_{23} \\ \Delta\epsilon_{31} \end{Bmatrix} \quad \ldots\ldots \quad (16)$$

in which $D_1 = (K + 4G/3)_{r-(1/2)}$; $D_2 = (K - 2G/3)_{r-(1/2)}$, and $D_3 = 2G_{r-(1/2)}$. Because $\Delta\sigma''_{ij}$ and the elastic coefficient matrix in Eq. 16 are known, one has a quasi-elastic incremental stress-strain law and the increments, $\Delta\sigma_{ij}$ and $\Delta\epsilon_{ij}$, in all finite elements may be solved by an elastic analysis of the structure. In case of specimens in a homogeneous state one just solves the six equations represented by Eq. 16.

6. Steps 2-5 are iterated using the increment values from the previous iteration, until the new values of Δz and $\Delta\lambda$ do not differ from the previous values for the same step by more than about 0.1%. If more than four iterations are required, it is better to decrease the size of step.

A theoretical investigation of convergence of this algorithm is difficult in general. However, for the case of uniaxial deformation with $f = F = 1$, it is easy to show that the iterates of $\Delta\epsilon$ for prescribed $\Delta\sigma$ represent sums of a geometric progression whose quotient equals $\Delta\epsilon''/\Delta\epsilon$. Therefore, convergence is assured when $\Delta\epsilon'' < \Delta\epsilon$, i.e., on the whole rising branch. The peak stress and the declining branch can be calculated only when $\Delta\epsilon$ is specified. For multiaxial stress and the actual functions, f and F, the convergence properties seem to be alike.

In similarity to previous developments for creep (4,8,9), the limit on the step size may be increased by using incremental relations based on exact integrals of the differential equation (Eqs. 6) obtained under the simplifying assumption that e_{ij}, ϵ, λ, and ϵ^0 vary linearly with z and t within the step. The integrals of Eqs. 6 are then of the form $\sigma = A + Be^{-(t-t_{r-1})/\tau_1}$, $s_{ij} = A_{ij} + B_{ij}e^{-(z-z_{r-1})}$ in which A, B, A_{ij}, and B_{ij} are constants. Imposing the initial conditions $\sigma = \sigma_{r-1}$, $s_{ij} = s_{ij_{r-1}}$, $\epsilon = \epsilon_{r-1}$, and $e_{ij} = e_{ij_{r-1}}$ at $t = t_{r-1}$, incremental quasielastic relations with the following values result:

$$\Delta\sigma'' = \sigma_{r-1}(1 - e^{-\Delta t/\tau_1}); \quad \Delta s''_{ij} = s_{ij_{r-1}}(1 - e^{-\Delta z}) \quad \ldots\ldots\ldots\ldots \quad (17)$$

$$K'' = K_{r-(1/2)}\frac{\tau_1}{\Delta t}(1 - e^{-\Delta t/\tau_1}); \quad G'' = G_{r-(1/2)}\frac{1}{\Delta z}(1 - e^{-\Delta z}) \quad \ldots\ldots\ldots \quad (18)$$

These values replace $\Delta\sigma_{ij}$, K, and G in setting up Eq. 16. Note that for $\Delta z \to 0$ and $\Delta t \to 0$, Eqs. 17 and 18 are equivalent to steps 5 and 6. Eqs. 17 and 18 are analogous to those derived in Ref. 9 for age-dependent viscoelastic behavior. Noting that $1 - e^{-\Delta z}$ and $1 - e^{-\Delta t/\tau_1}$ are bounded no matter how large Δz and Δt are, one can prove that numerical stability is independent of Δz and Δt. (Extension to the more general case of Eqs. 22 can be made similarly to Ref. 9.)

Identification of Material Parameters from Test Data

To identify material parameters from test data, a FORTRAN IV program based on the foregoing numerical algorithm has been written. For given values of material parameters, the program computes the responses to the stress or strain history inputs as prescribed for various particular types of tests. The test specimen is presumed to be in a homogeneous state of stress and strain, so that merely an integration of stress-strain relations is to be carried out

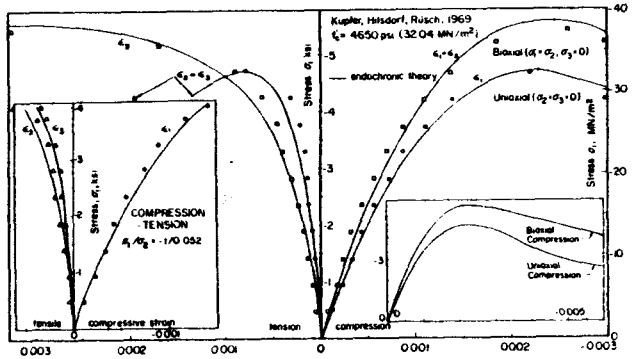

FIG. 3.—Fit of Biaxial Stress-Strain Data (26) with Lateral Strains

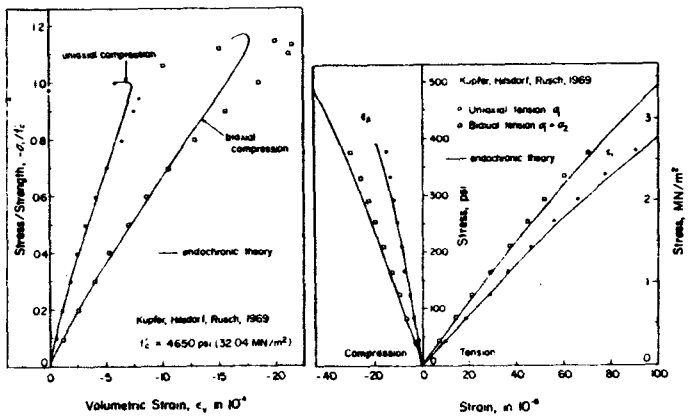

FIG. 4.—Fit of Data (26) on Volume Change in Uniaxial and Biaxial Compression and of Tensile Uniaxial and Biaxial Test Data (26)

An automatic plotting of response curves (by Calcomp plotter or by simulation on the printer) has been used on the output.

The values of material parameters are first arbitrarily varied to learn which parameter affects what. Then, by trial-and-error approach, the values of material parameters which give a qualitative agreement with known test results are found. Finally, the whole program may be arranged as a subroutine which computes

the deviations of the response curves from the specified data points. This subroutine is then hooked to a main program which calls a standard library optimization subroutine (modified Marquardt algorithm or the Powell method) for minimizing a sum of squares of nonlinear functions (the deviations) without computing the derivatives with respect to the unknown parameters. The optimiza-

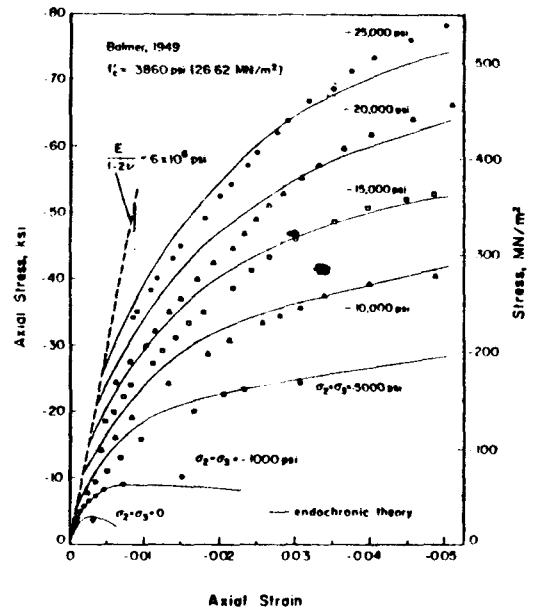

FIG. 5.—Fit of Triaxial Test Data (2)

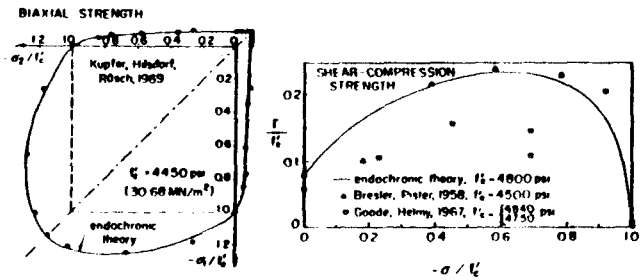

FIG. 6.—Fit of Biaxial Failure Envelope (26) (Same Test Series as Fig. 3) and of Torsion-Compression Failure Data (16,19)

tion subroutine automatically varies the material parameters until the optimum fit of test data is found. However, the optimization process converges to the true optimum (rather than a local optimum) only if the starting values of material parameters are sufficiently good estimates, and determination of these values, which must be done by trial-and-error approach, is by far the most tedious part of the whole endeavor.

Interchangeable subroutines have been used to generate the input values for various particular types of tests (e.g., biaxial compression, triaxial test). From each pair of values $(\Delta\epsilon_{ij}, \Delta\sigma_{ij})$, one value is prescribed and the other one is unknown (or a relationship between the two is given, as in the case of lateral confinement by a steel spiral). The subroutine rearranges the terms in the six algebraic equations defined by Eq. 16, in order to place all prescribed terms and all σ''_{ij} on the right-hand side and all unknown terms on the left-hand side. As an example, consider the biaxial test in which the strain increments, $\Delta\epsilon_{11}$, are prescribed and $\Delta\epsilon_{22} = k\Delta\epsilon_{11}$, with k = given constant, while $\sigma_{33} = \sigma_{12} = \sigma_{23} = \sigma_{31} = 0$; rearrangement of Eq. 16 then provides

$$\begin{bmatrix} -1 & 0 & D_2 & 0 & 0 & 0 \\ 0 & -1 & D_2 & 0 & 0 & 0 \\ 0 & 0 & D_1 & 0 & 0 & 0 \\ 0 & 0 & 0 & D_3 & 0 & 0 \\ 0 & 0 & 0 & 0 & D_3 & 0 \\ 0 & 0 & 0 & 0 & 0 & D_3 \end{bmatrix} \begin{Bmatrix} \Delta\sigma_{11} \\ \Delta\sigma_{22} \\ \Delta\epsilon_{33} \\ \Delta\epsilon_{12} \\ \Delta\epsilon_{23} \\ \Delta\epsilon_{31} \end{Bmatrix} = \begin{Bmatrix} \Delta\sigma''_{11} - (D_1 + kD_2)\Delta\epsilon_{11} \\ \Delta\sigma''_{22} - (D_2 + kD_1)\Delta\epsilon_{11} \\ \Delta\sigma''_{33} - (1 + k)D_2\Delta\epsilon_{11} \\ \Delta\sigma''_{12} \\ \Delta\sigma''_{23} \\ \Delta\sigma''_{31} \end{Bmatrix} \quad (19)$$

and this equation is solved at each step (item 5 of the foregoing algorithm). Similar equations have been set up for strain-controlled uniaxial tests (in which $\Delta\epsilon_{11}$ is specified and $\Delta\sigma_{22} = \Delta\sigma_{33} = \Delta\sigma_{12} = \Delta\sigma_{23} = \Delta\sigma_{31} = 0$); triaxial tests (in which hydrostatic pressure is applied first and subsequently $\Delta\epsilon_{11}$ is incremented keeping $\Delta\sigma_{22} = \Delta\sigma_{33} = \Delta\sigma_{12} = \Delta\sigma_{23} = \Delta\sigma_{31} = 0$); shear (torsion)-compression tests (in which $\Delta\epsilon_{31} = k\Delta\epsilon_{11}$, $\Delta\epsilon_{11}$, k being prescribed, and $\Delta\sigma_{22} = \Delta\sigma_{33} = \Delta\sigma_{12} = \Delta\sigma_{23} = 0$); and stress-controlled uniaxial tests, such as the cyclic compression test.

For describing axial tests of sprially reinforced cylinders (Fig. 10), one must substitute in Eq. 16 the relations, $\Delta\sigma_{22} = -E_s\rho_2\Delta\epsilon_{22}$, $\Delta\sigma_{33} = -E_s\rho_3\Delta\epsilon_{33}$, in which E_s = elastic modulus of steel; and $\rho_2 = \rho_3$ = spiral ratio (the ratio of cross-sectional areas of spiral and concrete in axial sections of a cylinder). Then, after inserting $\Delta\sigma_{12} = \Delta\sigma_{23} = \Delta\sigma_{12} = 0$, the equations forming Eq. 16 are rearranged so as to include on the left-hand side as unknowns only the quantities $\Delta\sigma_{11}$, $\Delta\epsilon_{22}$, $\Delta\epsilon_{33}$, $\Delta\epsilon_{12}$, $\Delta\epsilon_{23}$, and $\Delta\epsilon_{13}$; the controlled quantity is $\Delta\epsilon_{11}$. In case of prestressed spirals (Fig. 10), the calculation of axial test is preceded by a calculation of biaxial loading with prescribed $\Delta\epsilon_{22} = \Delta\epsilon_{33}$ and $\Delta\sigma_{11} = 0$, until the specified level of prestress is reached.

In cases with a large number of load cycles, the log N-scale (N = number of cycles) was subdivided by points $N = 3, 30, 300, \ldots, 3 \times 10^6$ cycles into intervals and the response cycle beyond the third cycle was computed only for load cycles $N = 3\sqrt{10}, 30\sqrt{10}, \ldots$ (the midpoints of intervals in log-scale), rounded as $N = 9, 95, 949, \ldots 948, 700$. Assuming that cycle $N = 3 \times 10^n\sqrt{10}$ gives the average value of $d\epsilon''_{11}/d(\log N)$. for the interval $(3 \times 10^n, 3 \times 10^{n+1})$, $\Delta\epsilon''$ per interval was obtained as (log 10) $d\epsilon''_{11}/d(\log N)$. Calculation of each interval was iterated several times with improved values of ϵ''_{11} and z for the midcycle of the interval.

The failure envelopes were constructed by running a number of cases (e.g., for various proportionality factors in biaxial tests) and collecting the peak points.

This agrees with the method used by experimentalists themselves in constructing the failure envelopes from test results. However, it should be kept in mind that this method need not give the correct failure loads for specimens very much larger than the aggregate size (13), which may fail by brittle fracture or by unstable propagation of a slip plane.

Note that for step-by-step structural analysis, a check for the peak value of load (or the point where the incremental stiffness matrix turns singular) is at least as simple as the use of some separate failure criterion. It is also more rational because the dependence of the failure criterion on stress path, well established for concrete, is automatically accounted for.

Fits of various experimental data available in the literature are indicated in

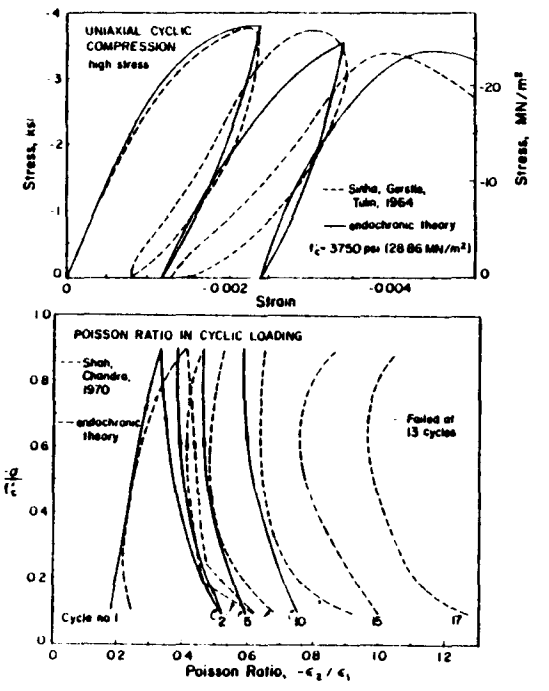

FIG. 7.—Fits of Uniaxial Cyclic Compression Data with Lateral Strains (41,42)

Figs. 2-10 by solid lines. Because for no single concrete complete data sets exist, it was inevitable to assume that some material parameters are the same for all standard-weight concretes. It is remarkable that among the parameters for short-time response only one, i.e., the cylindrical strength, f'_c, had to be varied from one data set to another. All remaining parameters are the same for all fits in Figs. 2-10 and their values are

$Z_1 = 0.0015$; $\beta_1 = 30$; $\beta_2 = 3{,}500$; $a_0 = 0.7$; $a_1 = 0.6(f'_c)^{-1}$;

$a_2 = 1{,}400$; $a_3 = 500(f'_c)^{-3}$; $a_4 = 475(f'_c)^{-2}$; $a_5 = 0.8(f'_c)^{-2}$;

$a_6 = 0.055(f'_c)^{-3}$; $a_7 = 20$; $a_8 = 0.000125$; $a_9 = 0.0015$; $\lambda_0 = 0.001$;

$c_0 = 1.0$; $c_1 = 100(f'_c)^{-1}$; $c_2 = 0.0005$; $\nu = 0.18$;

$$E_0 = (0.565 \text{ psi} + 0.0001\, f'_c)\, 57{,}000\, \sqrt{f'_c}\ (\text{psi})^{-1/2} \quad \ldots\ldots\ldots\ldots\ldots\ldots \quad (20)$$

in which 1 psi = 6,895 N/m². Exponents having values 1/2 and 1/3 in Eqs. 9 and 10, and 2 and 3 in Eq. 12, have been also varied in searching for optimum fits.

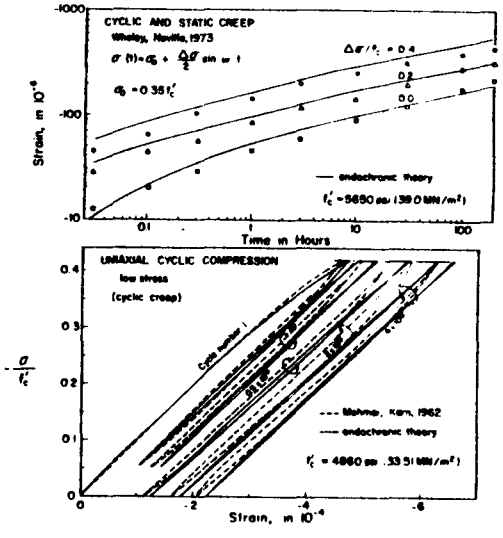

FIG. 8.—Fit of Cyclic Creep Tests (29,48)

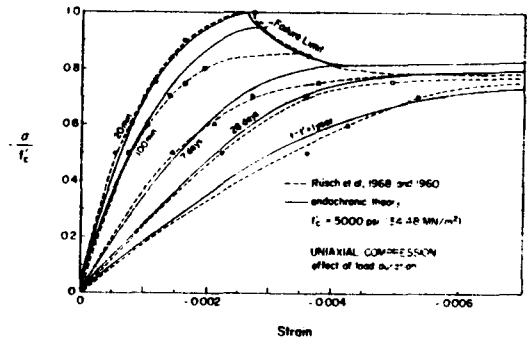

FIG. 9.—Fit of Data on Nonlinear Constant Stress Creep and Long-Time Failure (39)

The preceding formula for E_0 has been selected in order to give the optimum fit of the whole stress-strain curve. The E_0-value obtained from this formula often differs from the measured E_0-value; but the difference is very small, and so is the deviation from the ACI formula $E_0 = 57{,}000\, \sqrt{f'_c}$. The peak, $f'_{c,\text{output}}$, of the uniaxial stress-strain curve calculated from the values in Eq. 20 may deviate slightly (up to 2% between 3,500-psi and 6,000-psi strengths)

from the directly measured strength value, $f'_{c,\text{input}}$, used for f'_c in Eq. 20. It has been found that $f'_{c,\text{output}} = f'_c\{1{,}0025 + [(f'_c - 5{,}600)/12{,}000]^2\}$. By calculating f'_c from this formula, it would be possible to obtain the desired peak value exactly, but then the overall fit of the stress-strain curves would be impaired.

The obtained values of parameters τ_a and τ_b which characterize the time-dependent behavior have not been the same for different concretes, which is not surprising because creep does not possess a one-to-one relationship to strength. The following values have been found: $\tau_a = 1$ hr, $\tau_b = 20$ (Fig. 8); $\tau_a = 1$ day, $\tau_b = 2$ (Fig. 9); $\tau_a = 14.4$ hr, and $\tau_b = 0.75$ (Fig. 10).

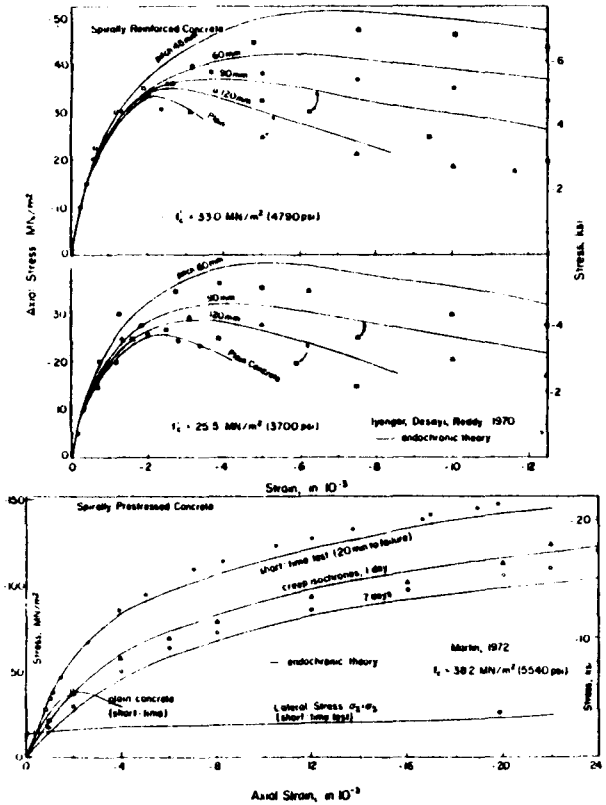

FIG. 10.—Fit of Axial Compression Tests of Spirally Reinforced Cylinders (21) and of Axial Compression and Creep of Spirally Prestressed Cylinders (28)

The test data in Figs. 2-10 cover all essential known features of multiaxial response of concrete and it is seen that they are all adequately modeled by one constitutive law. Moreover, one could show that this law also correctly predicts the strain rate effect on the stress-strain diagrams and the long-time strengthening of concrete due to low sustained compression stress. No constitutive law of comparable scope has been known thus far.

Although the beginning slope of the unloading branch is in concrete higher

than the initial tangent modulus, E_0, of the loading branch, it is often not quite as steep as the present theory indicates. An improvement is possible by replacing $d\xi$ with $k_0 d\xi$ whenever $dJ_2(\underline{\epsilon}) < 0$ (unloading criterion), k_0 being a positive constant less than one.

Strain-Softening Behavior.—From the stability point of view, there are certain difficulties in interpreting the declining branch of the $\sigma - \epsilon$ diagram (see Ref. 13). Nevertheless, inclusion of the declining branch into the range of the constitutive equation has important advantages. Firstly, by broadening the data range, the behavior on the rising branch near the stress peak can be identified more accurately from test data. Secondly, a smooth continuation through and beyond the peak stress point allows representing the failure by the $\sigma - \epsilon$ relation itself (rather than by a separate failure criterion, as usual), and this brings about automatically the dependence of failure upon the stress path.

Maxwell Chain Model for Nonlinear Long-Time Creep

For sufficiently small stress levels, $d\zeta$ is negligible in Eq. 4 and $dz \approx dt$, $d\lambda \approx 0$. In this limit case, Eqs. 6 are identical with the stress-strain law for the Maxwell solid. As is well known, Maxwell solid is insufficient to describe long-term creep, unless the artifice of time-hardening is adopted. However, this violates the principle of objectivity of the material and is inapplicable when the stress strongly varies in time. Correctly, the long-term creep may be characterized by a Maxwell chain (6,9) and the stress-strain relations must reduce to those for Maxwell chain when $d\zeta \approx 0$ and $d\lambda = 0$. This condition can be met by considering that each Maxwell unit of the chain is characterized by its own intrinsic time z_μ, which is given by Eq. 4 with τ_1 replaced by τ_μ, the relaxation time of the μth Maxwell unit. A proper choice is $\tau_\mu = \tau_1 10^{\mu-1}$ (6,9).

To examine whether it may be possible to use a simpler expression, $z_\mu = z/\tau_\mu$, in which z is a single intrinsic time defined by Eq. 4, consider that the time range of significant creep spans over many orders of magnitude of time (10^{-3} days–10^4 days), while the range of ζ in which nonlinearity occurs is narrow (about 10^{-4}–10^{-1}). Consequently, Eq. 4 would yield $z \approx \zeta/Z_1$ for $t < 0.2\ t_1$ and $z \approx t/\tau_1$ for $t > 2t_1$, t_1 being a certain time. Thus, except for a narrow time range, either the material would exhibit no creep or it would be linearly viscoelastic. This consequence is incorrect. Thus, a single intrinsic time cannot be used.

To model the nonlinear long-time creep, the definition of distorsion measure, ξ, must further be generalized so as to exclude the linearly viscoelastic parts of inelastic strains, de'_{ij}, for otherwise ξ would increase (and would thereby cause nonlinearity) even at the low-stress creep, which is known to be linear in stress and unrelated to microcracking or damage.

To sum up, Eqs. 5, 7, and 4 must now be generalized as follows:

$$d\xi_\mu = \left\{ \frac{1}{2}\, de^0_{ij}\, de^0_{ij} \right\}^{1/2}; \quad de^0_{ij} = de_{ij} - de'_{ij}; \quad de'_{ij} = \frac{s_{ij}}{2G_\mu}\,\frac{dt}{\tau_\mu} \qquad (21)$$

$$d\eta_\mu = F(\underline{\epsilon}, \underline{\sigma})\, d\xi_\mu; \quad d\xi_\mu = \frac{d\eta_\mu}{f(\eta_\mu)} \qquad (22)$$

$$dz_\mu = \left[\left(\frac{d\zeta_\mu}{Z_\mu} \right)^2 + \left(\psi_\mu \frac{dt}{\tau_\mu} \right)^2 \right]^{1/2}; \quad \mu = 1, 2, \ldots, n \qquad (23)$$

in which subscript μ has been appended to ξ, η, and ζ; and F and f are the same as before. Extending the stress-strain relations for Maxwell chain by the inclusion of z_μ, one has

$$2G_\mu\, de_{ij} = ds_{ij_\mu} + s_{ij_\mu}\, dz_\mu; \quad s_{ij} = \sum_{\mu=1}^{n} s_{ij_\mu};$$

$$3K_\mu(d\epsilon - d\lambda - d\epsilon^0) = d\sigma_\mu + \sigma_\mu \frac{dt}{\tau_\mu}; \quad \sigma = \sum_{\mu=1}^{n} \sigma_\mu \qquad (24)$$

in which G_μ and K_μ = the shear and bulk moduli associated with the μth Maxwell unit of the chain; and s_{ij_μ} and σ_μ = the hidden stresses associated with the μth unit. Moduli G_μ K_μ are age-dependent (4,6,9). The volumetric relation in Eq. 24 involves again dt rather than dz_μ because there can be no inelastic decrease of volume due to microcracking or slip.

The short-time nonlinear deformations have been described herein satisfactorily by a model corresponding to a single Maxwell unit (Eqs. 6). Such a limiting case of Eqs. 24 would be obtained for $dt = 0$ only if all Z_μ-values were approximately the same. However, it seems that Z_μ should increase with μ ($\mu = 1, 2, \ldots n$), for if it did not the long-term creep would exhibit much stronger nonlinearity than the short-time deformation, by virtue of the fact that ξ_μ and ζ_μ can reach after long-term creep much larger values. Parameters ψ_μ must reduce to 1.0 when the stress level is low, so as to obtain the correct linear viscoeleastic model as the limit; possibly all ψ_μ can be taken equal to one.

It has been tried to fit the present data with a standard-solid type model (Maxwell unit parallel to a spring). This allowed slightly better description of the first unloading but made $d\epsilon''$ much too small after a number of cycles.

Derivation from Hereditary Integrals.—Logically, it is quite natural to begin with the assumption that the stress tensor is a quasilinear functional of the history of the strain tensor. In view of isotropy, this assumption may be stated as

$$s_{ij}(t) = 2\int_{t_0}^{t} \bar{G}(t, t')\, de_{ij}(t');$$

$$\sigma(t) = 3\int_{t_0}^{t} \bar{K}(t, t')[d\epsilon(t') - d\lambda(t') - d\epsilon^0(t')] \qquad (25)$$

in which $\bar{G}$ and $\bar{K}$ are kernels analogous to the relaxation functions (4). It is well known (4,6,9) that the kernels can be approximated with any desired accuracy by sums of exponentials. Noting that the independent variables in which the functionals become quasilinear are z_μ and t, these sums may be written (similarly to Ref. 4) as $\bar{G}(t, t') = \Sigma_\mu\, G_\mu(t') \exp\,[-z_\mu(t) + z_\mu(t')]$; $\bar{K}(t, t') = \Sigma_\mu\, K_\mu(t') \exp\,[-(t - t')/\tau_\mu]$. After substitution, Eq. 25 may be cast in the form:

$$s_{ij} = \sum_\mu s_{ij_\mu}; \quad s_{ij_\mu}(t) = 2\int_{t_0}^{t} G_\mu(t')\, e^{-z_\mu(t)+z_\mu(t')}\, de_{ij}(t'); \quad \sigma = \sum_\mu \sigma_\mu;$$

$$\sigma_\mu(t) = 3\int_{t_0}^{t} K_\mu(t')\, e^{-(t-t')/\tau_\mu}\,[d\epsilon(t') - d\lambda(t') - d\epsilon^0(t')] \quad \ldots\ldots\ldots \quad (26)$$

Now, substituting $de_{ij} = (de_{ij}/dz_\mu)(dz_\mu/dt')dt'$, and inserting Eq. 26 into Eqs. 24, one finds that Eqs. 24 are identically satisfied. Conversely, Eqs. 26 represent the integral of Eqs. 24. Thus, Eqs. 24, as well as Eqs. 6, follow logically from a rather plausible and general assumption about the functional dependence.

Remark on Variable Temperature and Humidity.—The Maxwell chain model has been formulated in previous work to describe linear creep of aging concrete at variable temperature (10), as well as creep and shrinkage at variable humidity (11) along with the nonlinearities due to drying. These generalizations, which have been carried out only for the low stress range, can also be made for the present formulation having no stress range limitation.

Conclusions

The endochronic theory for nonlinear behavior of concrete provides a rather complete model which is far better than other constitutive laws known thus far. As compared with the previous formulation of the endochronic theory for metals, three major extensions are necessary in order to model: (1) The hydrostatic pressure sensitivity of inelastic strain; (2) the inelastic dilatancy; and (3) the strain-softening tendency at high stress. By virtue of the last extension, the theory at the same time provides the failure criterion, in which its dependence on strain and stress paths is automatically accounted for. Furthermore, a number of different intrinsic times should be considered when dealing with nonlinear long-time creep.

Acknowledgment

Development of the general theory has been funded under National Science Foundation Grants GK-26030 and ENG 75-14848, and the material identification has been sponsored by the Energy Research and Development Administration through Oak Ridge National Laboratory under contract with Union Carbide Corporation. Sia Nemat-Nasser of Northwestern University is thanked for suggesting the use of Valanis' endochronic theory as the point of departure.

Appendix I.—Additional Information on Test Data Used

For *Fig. 2*: 6-in. × 12-in. cylinders, age 14 days, type I cement, Elgin sand and gravel, 1-1/2-in. maximum size, moist cured, then 5 days drying at 75° F and 50%-80% relative humidity. For *Fig. 3*: Constant ϵ_1, maximum load reached in ≈20 min; brush-bearing platens; slabs 20 cm × 20 cm × 5 cm, 28 days old; moist cured 7 days, then drying at 65% relative humidity and 78° F; 190 kg of cement per cubic meter of concrete, gravel maximum size 15 mm. For *Fig. 5*: 6-in. × 12-in. cylinders, water-cement-sand-gravel ratio 0.58:1:2.86:4.47, cement type II, Grand Coulee aggregate maximum size 1.5 in., fog-cured 28 days at 70° F, then oven-dried; hydrostatic pressure applied first, then axial load superimposed. For *Fig. 6*: In torsion tests, compression applied first, then torsion to failure. *Ref. 16*: Hollow cylinders 9 in. × 30 in., 1.5-in. thick, 28

days old, type I cement, water-cement-sand-gravel ratio 0.52:1:2.92:3.57, river gravel maximum size 0.5 in. *Ref. 19*: Hollow cylinders 8 in. × 36 in. hollow on 26-in. length, 1-in. walls, type I cement, water-cement-sand-gravel ratio 0.45:1:1.6:2.4, river gravel maximum size 3/8 in., unmolded at 28 days, cured in shower for 5 days at 66° F. For *Fig. 7*; *Ref. 40*: 6-in. × 12-in. cylinders, fog-cured for 28 days, then drying at room temperature, capped, and tested at age 2 months-4 months, 1 cycle/min. *Ref. 39*: Prisms 4 in. × 4 in. × 12 in., Type I cement, water-cement-sand-gravel ratio 0.54:1:2:4, aggregate maximum size 3/4 in.; tested after 14 days of moist curing; 4 cycles/min. For *Fig. 8*; *Ref. 27*: 15-cm × 60-cm cylinders, water-cement-aggregate ratio 0.44:1:4.5, drying at 65% relative humidity; cube strength 498 kgf/cm²; after 20 slow cycles (completed within a few minutes), 380 cycles/min. *Ref. 46*: Prisms 76 mm × 76 mm × 203 mm, water-cement-sand-gravel ratio 0.5:1:2:4; quartzite gravel, 10-mm maximum size; fog cured at 20° C for 14 days; 585 cycles/min; first a slow cycle to the limit stress, then rapid cycling with amplitude growing from 0 gradually over first 500 cycles, zero time = 250th cycle. For *Fig. 9*: Prisms 10 cm × 15 cm × 60 cm with widened ends, water-cement-aggregate ratio 0.55:1:4.9; Rhine gravel (mostly quartz); 28-day cube strength 350 kgf/cm², moist cured for 7 days at 20° C, then drying at 65% relative humidity, 20° C, loading rate—20 min to failure. For *Fig. 10*; *Ref. 21*: Cylinders 150 mm × 300 mm, ordinary Portland Cement, granite aggregate, 18-mm maximum size, river sand. Mix 1:water-cement-sand-gravel ratio 0.5:1:1.5:3, f'_c = 25.5 N/mm². Mix 2: ratio 0.4:1:1:2, f'_c = 33.0 N/mm². Cured 28 days in water, then drying, cool storage, tested at 45-day age. Spirals 6.5-mm diam, yield strength 319 N/mm²; ρ = 0.738, 0.983, 1.475, 1.965 for pitch from 45 mm–120 mm. *Ref. 28*: Cylinders 3 in. × 12 in., Platte River Valley sand and gravel, water-cement-aggregate ratio 0.53:1:5.34, moist cured for 18 days, then drying; winding at 24-day age by wire of 0.51-mm diam, pitch 0.56 mm, ρ = 0.019, initial wire tension 1600 N/mm² (232 ksi) producing lateral stress 14.48 N/mm² (2.10 ksi). Start of test at 40-day age, strength 38.2 N/mm² (5.54 ksi) at start of test. Loaded at strain rate 0.01/10 min, followed by constant-load creep.

Appendix II.—References

1. Argyris, J. H., et al., "Recent Developments in the Finite Element Analysis of Prestressed Concrete Reactor Vessels," *Nuclear Engineering and Design*, Vol. 28, 1974, 42-75; see also *Report No. 151*, Institute für Statik und Dynamik, University of Stuttgart, Stuttgart, Germany, 1973.
2. Balmer, G. G., "Shearing Strength of Concrete under High Triaxial Stress—Computation of Mohr's Envelope as a Curve," *Sturctural Research Laboratory Report No. SP-23*, Denver, Colo., Oct., 1949.
3. Bažant, Z. P., "A New Approach to Inelasticity and Failure of Concrete, Sand, and Rock: Endochronic Theory" (Abstract), *Proceeding*, Society of Engineering Science, 11th Annual Meeting, G. J. Dvorak, ed., Duke University, Durham, N.C., Nov., 1974, pp. 158-159.
4. Bažant, Z. P., "Theory of Creep and Shrinkage in Concrete Structures: A Précis of Recent Developments," *Mechanics Today*, Vol. 2, S. Nemat-Nasser, ed., Pergamon Press, Inc., New York, N.Y., 1975, pp. 1-93.
5. Bažant, Z. P., and Asghari, A., "Computation of Kelvin Chain Retardation Spectra of Aging Concrete," *Cement and Concrete Research*, Vol. 4, 1974, pp. 797-806.
6. Bažant, Z. P., and Asghari, A., "Computation of Age-Dependent Relaxation Spectra," *Cement and Concrete Research*, Vol. 4, 1974, pp. 567-579.

7. Bažant, Z. P., and Najjar, L. J., "Comparison of Approximate Linear Methods for Concrete Creep," *Journal of the Structural Division*, ASCE, Vol. 99, No. ST9, Proc. Paper 10006, Sept., 1973, pp. 1851-1874.
8. Bažant, Z. P., and Wu, S. T., "Dirichlet Series Creep Function for Aging Concrete," *Journal of the Engineering Mechanics Division*, ASCE, Vol. 99, No. EM2, Proc. Paper 9645, Apr., 1973, pp. 367-387.
9. Bažant, Z. P., and Wu, S. T., "Rate-Type Creep Law of Aging Concrete Based on Maxwell Chain," *Materials and Structures*, Vol. 7, No. 37, Jan-Feb., 1974, pp. 45-60.
10. Bažant, Z. P., and Wu, S. T., "Thermoviscoelasticity of Aging Concrete," *Journal of the Engineering Mechanics Division*, ASCE, Vol. 100, No. EM3, Proc. Paper 10621, June, 1974, pp. 575-597.
11. Bažant, Z. P., and Wu, S. T., "Creep and Shrinkage Law of Concrete at Variable Humidity," *Journal of the Engineering Mechanics Division*, ASCE, Vol. 100, No. EM6, Proc. Paper 10995, Dec., 1974, pp. 1183-1209.
12. Bažant, Z. P., "Some Questions of Material Inelasticity and Failure in the Design of Concrete Structures for Nuclear Reactors," *Transactions*, 3rd International Conference on Structural Mechanics in Reactor Technology, London, United Kingdom, Vol. 3, Paper H1/1, Sept., 1975.
13. Bažant, Z. P., "Instability, Ductility and Size Effect in Strain-Softening Concrete," *Journal of the Engineering Mechanics Division*, ASCE, Vol. 102, No. EM2, Proc. Paper 12042, Apr., 1976, pp. 331-344.
14. Bennett, E. W., and Raju, N. K., "Cumulative Fatigue Damage of Plain Concrete in Compression," *Proceedings of the Symposium on Structure, Solid Mechanics and Engineering Design*, 1969, University of Southampton, Southampton, England, pp. 1089-1102, ed. by M. Te'eni, John Wiley and Sons, Inc., New York, N.Y., 1971.
15. Bresler, B., and Pister, K. S., "Failure of Plain Concrete under Combined Stresses," *Proceedings*, ASCE, Vol. 81, Separate No. 674, Apr., 1955, pp. 674-1-674-17.
16. Bresler, B., and Pister, K. S., "Strength of Concrete under Combined Stresses," *American Concrete Institute Journal*, Vol. 551, Sept., 1958, pp. 321-345.
17. Červenka, V., and Gerstle, K. H., "Inelastic Analysis of Reinforced Concrete Panels," *Publications*, International Association for Bridge and Structural Engineering, Zurich, Switzerland, Vol. 31, 1971, pp. 31-45, and Vol. 32, 1972, pp. 25-39.
18. Coon, M. D., and Evans, R. J., "Incremental Constitutive Laws and their Associated Failure Criteria with Application to Plain Concrete," *International Journal of Solids and Structures*, Vol. 8, 1972, pp. 1169-1183.
19. Goode, C. D., and Helmy, M. A., "The Strength of Concrete under Combined Shear and Direct Stress," *Magazine of Concrete Research*, Vol. 19, No. 59, June, 1967, pp. 105-112.
20. Hognestad, E., Hanson, N. W., and McHenry, D., "Concrete Stress Distribution in Ultimate Strength Design," *American Concrete Institute Journal*, Vol. 52, No. 4, Dec., 1955, pp. 455-477.
21. Iyengar, K. T. S., Desayi, P., and Reddy, K. N., "Stress-Strain Characteristics of Concrete Confined in Steel Binders," *Magazine of Concrete Research*, Vol. 22, No. 72, Sept., 1970, pp. 173-184.
22. Ilyushin, A. A., "On the Relation Betwen Stresses and Small Deformations in the Mechanics of Continuous Media, *Prikladnaya Matematika i Mekhanika*, Vol. 18, 1954, pp. 641-666, (in Russian).
23. Kupfer, H. B., "Das Verhalten des Betons unter mehrachsiger Kurzzeitbelastung unter besonderer Berücksichtigung der zweiachsigen Beanspruchung," *Deutcher Ausschuss für Stahlbeton*, Heft 229, W. Ernst & Sohn, Berlin, Germany, 1972.
24. Kupfer, H. B., "Das nicht-lineare Verhalten des Betons bei Zweiachsiger Beanspruchung," *Beton-und Stahlbetonbau*, Vol. 11, 1973, pp. 269-274.
25. Kupfer, H. B., and Gerstle, K. H., "Behavior of Concrete Under Biaxial Stresses," *Journal of the Engineering Mechanics Division*, ASCE, Vol. 99, No. EM4, Proc. Paper 9917, Aug., 1973, pp. 853-866.
26. Kupfer, H., Hilsdorf, H. K., and Rüsch, H., "Behavior of Concrete Under Biaxial Stresses," *American Concrete Institute Journal*, Vol. 66, Aug., 1969, pp. 656-666.
27. Liu, T. C. Y., Nilson, A. H., and Slate, F. O., "Biaxial Stress-Strain Relations

for Concrete," *Journal of the Structural Division*, ASCE, Vol 98, No. ST5, Proc. Paper 8905, May, 1972, pp. 1025-1034.
28. Martin, C. W., "Creep in Spirally Prestressed Concrete Cylinders," *Journal of American Concrete Institute*, Vol. 69, Apr., 1972, pp. 224-232.
29. Mehmel, A., and Kern, E., "Elastische and plastische Stauchungen von Beton infolge Druckschwell-und Standbelastung," *Deutscher Auschuss für Stahlbeton*, Heft 153, W. Ernst & Sohn, Berlin, Germany, 1962.
30. Nemat-Nasser, S., "On Nonequilibrium Thermodynamics of Continua," *Mechanics Today*, S. Nemat-Nasser, ed., Vol. 2, Pergamon Press, Inc., New York, N.Y., 1975, pp. 94-158.
31. Nilson, A. H., "Nonlinear Analysis of Reinforced Concrete by Finite Elements," *American Concrete Institute Journal*, Vol. 65, 1968, pp. 757-766.
32. Palaniswamy, R., and Shah, S. P., "Fracture and Stress-Strain Relationship of Concrete under Triaxial Compression," *Journal of the Structural Division*, ASCE, Vol. 100, No. ST5, Proc. Paper 10547, May, 1974, pp. 901-916.
33. Pipkin, A. C., Rivlin, R. S., "Mechanics of Rate-independent Materials," *ZAMP*, Vol. 16, 1965, pp. 313-327.
34. Richart, F. E., Brandtzaeg, A., and Brown, R. L., "A Study of the Failure of Concrete Under Combined Compressive Stresses," *Bulletin No. 185*, University of Illinois Engineering Experiment Station, Nov., 1928, pp. 1-73.
35. Richart, F. E., Brandtzaeg, A., and Brown, R. L., "The Failure of Plain and Spirally Reinforced Concrete in Compression," *Bulletin No. 190*, University of Illinois Engineering Experiment Station, Apr., 1929, pp. 1-103.
36. Rashid, Y. D., "Nonlinear Analysis of Two-Dimensional Problems in Concrete Creep," *Journal of Applied Mechanics, Transactions*, American Society of Mechanical Engineers, Vol. 39, 1972, pp. 475-482.
37. Rivlin, R. S., "Nonlinear Viscoelastic Solids," *Society for Industrial and Applied Mechanics Review*, Vol. 7, 1965, pp. 323-340.
38. Romstad, K. M., Taylor, M. A., Hermann, L. R., "Numerical Biaxial Characterization for Concrete," *Journal of the Engineering Mechanics Division*, ASCE, Vol. 100, No. EM5, Proc. Paper 10879, Oct., 1974, pp. 935-948.
39. Rüsch, H., "Researches toward a General Flexural Theory for Structural Concrete," *American Concrete Institute Journal*, Vol. 57, 1960, pp. 1-28.
40. Scordelis, A. C., "Finite Element Analysis of Reinforced Concrete Structures," Speciality Conference on the Finite Element Methods in Civil Engrg., held at McGill University, Montreal, Quebec, Canada, 1972, pp. 71-113.
41. Shah, S. P., and Chandra, S., "Mechanical Behavior of Concrete Examined by Ultra-Sonic Measurements," *Journal of Materials*, American Society for Testing and Materials, Vol. 5, No. 3, 1970, pp. 550-563.
42. Sinha, B. P., Gerstle, K. H., and Tulin, L. G., "Stress-Strain Relations for Concrete under Cyclic Loading," *American Concrete Institute Journal*, Vol. 61, No. 2, Feb., 1964, pp. 195-210.
43. Suidan, M., Schnobrich, W. C., "Finite Element Analysis of Reinforced Concrete," *Journal of the Structural Division*, ASCE, Vol. 99, No. ST10, Proc. Paper 10081, Oct., 1973, pp. 2109-2122.
44. "Symposium on Inelasticity and Nonlinearity of Structural Concrete," M. Z. Cohn, ed., University of Waterloo Press, Waterloo, Ontario, Canada, 1973.
45. Valanis, K. C., "A Theory of Viscoplasticity without a Yield Surface," *Archiwum Mechaniki Stossowanej*, Vol 23, 1971, pp. 517-551.
46. Valanis, K. C., "Effect of Prior Deformation on Cyclic Response of Metals," *Journal of Applied Mechanics*, American Society for Mechanical Engineers, Vol. 41, 1974, pp. 441-447.
47. Valliappan, S., Doolan, T. F., Nonlinear Stress Analysis of Reinforced Concrete, *Journal of the Structural Division*, ASCE, Vol. 98, No. ST4, Proc. Paper 8845, Apr., 1972, pp. 885-898.
48. Whaley, C. P., and Neville, A. M., "Non-elastic Deformation of Concrete under Cyclic Compression," *Magazine of Concrete Research*, Vol. 25, No. 84, Sept., 1973, pp. 145-154.

12360 ENDOCHRONIC THEORY AND FAILURE OF CONCRETE

KEY WORDS: **Concrete; Concrete durability; Creep; Engineering mechanics; Failure;** Inelastic action; Nonlinear systems; Plasticity; Stress strain characteristics; Triaxial tests

ABSTRACT: A gradual accumulation of inelastic strain can be most conveniently described in terms of the so-called intrinsic time, whose increment depends on the time increment as well as the strain increments, and was previously developed for metals and is extended herein to concrete. It is demonstrated that the proposed model predicts quite closely: (1)Stress-strain diagrams for concretes of different strength; (2)uniaxial, biaxial, and triaxial stress-strain diagrams and failure envelopes; (3)failure envelopes for combined torsion and compression; (4)lateral strains and volume expansion in uniaxial and biaxial tests; (5)the behavior of spirally confined concrete; (6) hysteresis loops for repeated high compression; (7)cyclic creep up to 10^6 cycles; (8)the strain rate effect; (9)the decrease of long time strength; and (10)the increase of short-time strength due to low stress creep.

REFERENCE: Bazant, Zdenek P., and Bhat, Parameshwara D., "Endochronic Theory of Inelasticity and Failure of Concrete," *Journal of the Engineering Mechanics Division*, ASCE, Vol. 102, No. EM4, Proc. **Paper 12360**, August, 1976, pp. 701-722